Chemical Science

Accepted Manuscript

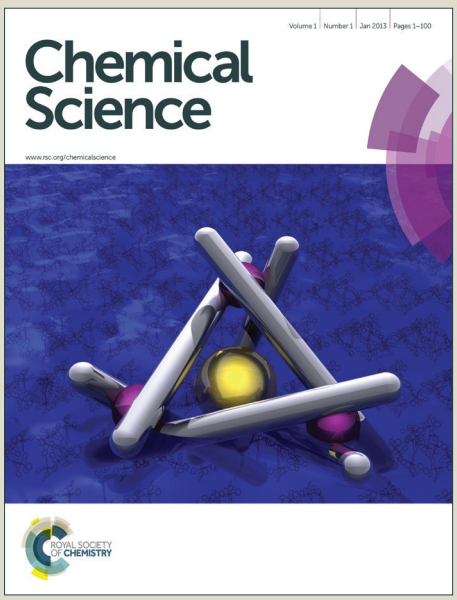

ROYAL SOCIETY OF CHEMISTRY

www.rsc.org/chemicalscience

Journal Name

ARTICLE

Unprecedentedly targeted customization of molecular energy levels with auxiliary-group in organic solar cell sensitizers†

Received 00th January 20xx,
Accepted 00th January 20xx

DOI: 10.1039/x0xx00000x

www.rsc.org/

Yongshu Xie,‡ Wenjun Wu,‡ Haibo Zhu, Jingchuan Liu, Weiwei Zhang, He Tian and Wei-Hong Zhu*

In dye-sensitized solar cells (DSSCs), the HOMO-LUMO energy gap of organic sensitizers should be large enough for enabling efficient electron injection and dye regeneration. However, the LUMOs of most practical organic dyes are always too high in making energy "waste". In order to deepen the LUMOs, we focus on the targeted modulation of molecular energy levels by embedding an electron donor or acceptor into the skeleton of typical D-π-A model. The electron-rich group of 3,4-ethylenedioxythiophene (EDOT) lifts up the HOMO level with little influence on the LUMO, while the electron-deficient group of benzothiadiazole (BTD) or benzooxadiazole (BOD) mainly casts down the customized LUMO level. As a consequence, the auxiliary group change from EDOT (Dye **WS-53**) to BOD (Dye **WS-55**) brings forth a huge photoelectric conversion efficiency (PCE) increase by 38 folds from 0.24 to 9.46% based on I^-/I_3^- redox couple, and even reaching a high PCE of 10.14% with **WS-55** under 0.3 sunlight irradiation.

Introduction

Dye sensitized solar cells (DSSCs) have received considerable attention due to their relatively high power conversion efficiency, low cost and high stability.[1-3] Enormous research passions have also be devoted to metal-free organic dyes because of their excellent photophysical properties.[4] Up to now, the donor-π bridge-acceptor (D-π-A) motif has been widely exploited for tailoring organic sensitizers.[5] Among them, introducing auxiliary groups in the skeleton of D-π-A system can exhibit a significant influence on the energy levels, light response, dye stability as well as photovoltaic performances in organic sensitizers.[6,7]

Generally, the LUMO and HOMO energy levels of organic sensitizers play important roles in electron injection and dye regeneration for DSSCs. Specifically, the driving force for electron injection from the excited dyes to TiO_2 conduction band (-0.5 V *vs.* NHE) should be greater than 0.2 V, and that for efficient dye regeneration from iodine electrolyte (0.4 V *vs.* NHE) should be greater than 0.3 V.[8] That is, the ideal LUMO and HOMO for an organic sensitizer should lie around -0.7 V and 0.7 V, respectively, with a proper band gap of about 1.4 eV. However, the LUMOs of most organic sensitizers actually used in DSSCs are too high, resulting in energy "waste". Given the basic injection dynamics, lowering the LUMO level and lifting the HOMO level in organic dyes can be expected to narrow the band gap ($E_{0\text{-}0}$) and extend light response, thus efficiently optimizing the photovoltaic performances of DSSCs. In this regard, the targeted customization of molecular energy levels is still a challenge.

With this in mind, we herein present a new series of dithieno[3,2-*b*:2',3'-*d*]pyrrole (DTP)-based organic sensitizers (Scheme 1) using different auxiliary groups in π-bridge. Based on the reference dye **WS-52**, an electron-rich unit of 3,4-ethylenedioxythiophene (EDOT) and electron-deficient groups of benzothiadiazole (BTD) and benzooxadiazole (BOD) were specifically introduced into **WS-53**, **WS-54** and **WS-55**, respectively. Interestingly, the embedding electron donor or acceptor can well customize the molecular energy levels. In distinct contrast with EDOT, the electron-deficient group of BTD or BOD mainly casts down the LUMO level, being capable of exactly preventing the energy waste in electron injection. Typically, the auxiliary group change from EDOT (Dye **WS-53**) to BOD (Dye **WS-55**) induced a large PCE increase of 38 folds from 0.24% to 9.46% based on I^-/I_3^- redox couple, and even reaching a high PCE of 10.14% with **WS-55** under 0.3 sunlight irradiation.

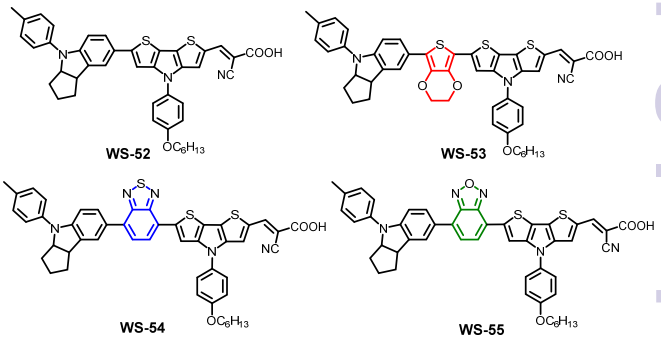

Scheme 1. Molecular structures of dyes **WS-52**, **WS-53**, **WS-54** and **WS-55** containing different auxiliary groups for targeted customization of molecular energy levels.

Key Laboratory for Advanced Materials and Institute of Fine Chemicals, Shanghai Key Laboratory of Functional Materials Chemistry, Collaborative Innovation Center for Coal Based Energy (i-CCE), East China University of Science & Technology, Shanghai 200237 (China). E-mail: whzhu@ecust.edu.cn

† Electronic Supplementary Information (ESI) available: Synthesis and characterization, and additional photovoltaic data. See DOI: 10.1039/x0xx00000x

‡ These authors contributed equally to this work.

Table 1. Photophysical and electrochemical properties of **WS-52**, **WS-53**, **WS-54** and **WS-55**, and their photovoltaic parameters of DSSCs.

Dyes	λ_{max}[a] (nm)	ε[a] (M^{-1} cm^{-1})	λ_{max}[b] (nm)	HOMO[c] (*V*)	$E_{0\text{-}0}$[d] (*V*)	LUMO[e] (*V*)	J_{SC} (mA cm^{-2})	V_{OC} (m*V*)	*FF*	η[f] (%)
WS-52	549	50160	461	0.75	2.02	-1.27	7.88±0.06	640±5	0.68±0.01	3.44±0.11
WS-53	570	33788	492	0.57	1.89	-1.32	1.22±0.12	440±8	0.48±0.03	0.24±0.06
WS-54	563	44514	530	0.81	1.83	-1.02	15.84±0.06	660±3	0.68±0.01	7.14±0.09
WS-55	558	35105	545	0.90	1.77	-0.87	19.66±0.47	678±5	0.70±0.02	9.46±0.19
WS-55[h]							6.74±0.08	643±3	0.73±0.01	10.05±0.09

[a] Absorption parameters were obtained in CH_2Cl_2. [b] Absorption parameters were obtained on 3 μm nanocrystalline TiO_2 film. [c] The HOMO was obtained in CH_2Cl_2 with ferrocene (0.63 V vs. NHE) as external reference. [d] $E_{0\text{-}0}$ values were estimated from the wavelength at 10% maximum absorption intensity for the dye-loaded 3 μm nanocrystalline TiO_2 film. [e] The LUMO was calculated according to LUMO = HOMO – $E_{0\text{-}0}$. [f] The efficiency was obtained from the average value of five devices. [h] The photovoltaic parameters were obtained under 0.3 sun light irradiation.

Results and discussion

The syntheses of dyes **WS-52**, **WS-53**, **WS-54** and **WS-55** are straightforward and described in the Electronic Supplementary Information (ESI†). Their absorption spectra in CH_2Cl_2 are depicted in Fig. 1a, and the corresponding data are summarized in Table 1. The reference dye **WS-52** shows two distinct absorption bands around 360 and 549 nm, corresponding to the π-π* and intramolecular charge transfer (ICT) transition bands, respectively. **WS-53** exhibits a significant bathochromic shift in the ICT band from 549 to 570 nm due to the extended π-conjugation with EDOT unit. Through inserting strong electron-withdrawing units of BTD and BOD, **WS-54** and **WS-55** exhibit bathochromic shifts by 14 and 9 nm, respectively. Compared with **WS-52**, insertion of the auxiliary group (electron-rich or deficient group) into the π-spacer leads to obvious red-shift of the ICT band in CH_2Cl_2. Upon adsorption onto TiO_2 films (Fig. 1b), all these four dyes show hypsochromic shifts due to the deprotonation of cyanoacrylic acid group (Table 1). **WS-52** and **WS-53** show large hypsochromic shifts by 88 nm from 549 to 461 nm and 78 nm from 570 to 492 nm, respectively. In contrast, **WS-54** and **WS-55** containing strong electron-withdrawing auxiliary-groups bestow much less hypsochromic shifts by 33 nm from 563 to 530 nm and 13 nm from 558 to 545 nm, respectively. Obviously, upon incorporation of strong electron withdrawing groups like BTD or BOD, the D-A-π-A featured **WS-54** and **WS-55** bring forth broader light response, contributed from the smaller hypsochromic shift onto TiO_2 and the presence of additional sub-absorption band in the region of 400-450 nm.[6b]

Next, we focus on the customized modulation of molecular energy levels by embedding the auxiliary electron donor or acceptor into the skeleton of typical D-π-A model. Based on the

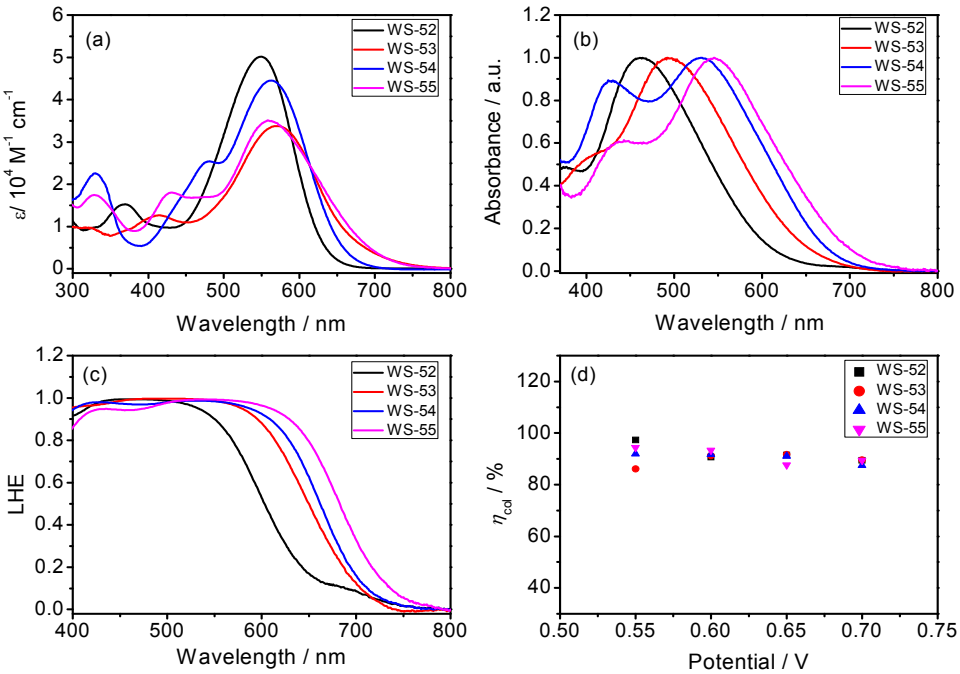

Fig. 1 Absorption spectra of **WS-52**, **WS-53**, **WS-54** and **WS-55** in CH_2Cl_2 solution (a) and coated onto 3 μm TiO_2 film (b), LHE spectra calculated from the absorption spectra of dye-loaded TiO_2 film (c), and charge collection efficiency (η_{col}) in DSSCs as the function of bias potentials during the EIS measurement (d).

cyclic voltammetry (Fig. 2a and Table 1), the first redox potentials corresponding to HOMO values are 0.75, 0.57, 0.81 and 0.90 V (vs. NHE) for dyes **WS-52**, **WS-53**, **WS-54** and **WS-55**, respectively. Due to the electron donating property of EDOT, the HOMO of **WS-53** is lifted by 0.18 V with respect to **WS-52**, and there exists only 0.17 V driving force for dye regeneration from iodine electrolyte (Fig. 2b).[8b] As estimated from HOMO and $E_{0\text{-}0}$ (Table 1), the LUMO values of **WS-52**, **WS-53**, **WS-54** and **WS-55** are -1.27, -1.32 -1.02 and -0.87 V, respectively. Interestingly, the auxiliary electron-rich EDOT group predominantly lifts up the HOMO level with little influence on the LUMO, while the electron-deficient BTD or BOD group mainly casts down the LUMO level. It is noteworthy that the stronger electron-withdrawing capability of BOD in **WS-55** dramatically lowers the LUMO orbital from -1.27 V (**WS-52**) to -0.87 V. With regard to these four dyes, the insertion of different pull or push auxiliary groups can provide an efficient channel to realize the targeted customization of HOMO and LUMO energy levels. Generally, the driving force for TiO_2 electron injection is always much larger than the minimum requirement because LUMOs of most organic sensitizers are always higher than -1.0 V. Comparing these four dyes, the customized LUMO orbital change from -1.27 V (reference **WS-52**), -1.02 V (**WS-54**) to -0.87 V (**WS-55**) gives a unprecedentedly preferable modulation, in which we can efficiently decrease the "waste" in electron-injection driving force, and thus efficiently decrease the HOMO-LUMO energy gap, resulting in the desirable light response in the long-wavelength range. Indeed, **WS-55** exhibited a long absorption onset wavelength as well as a promising PCE of 9.46% (Table 1), which is around 38 folds higher than dye **WS-53** (0.24%). In the following, we take insight into how the incorporated auxiliary groups of EDOT, BTD and BOD play such different role in photovoltaic performances, especially focusing on short-circuit current density (J_{SC}) and open-circuit voltage (V_{OC}).

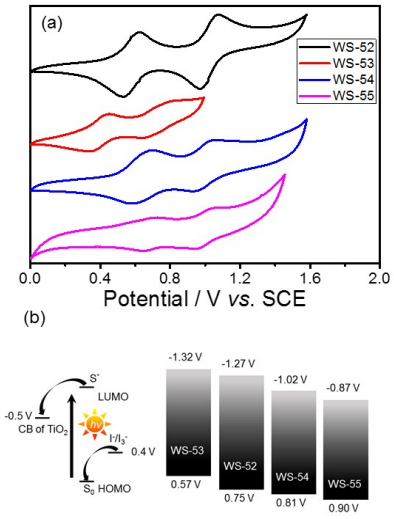

Fig. 2 (a) Cyclic voltammograms of **WS-52**, **WS-53, WS-54** and **WS-55** in CH_2Cl_2, and (b) schematic diagram of energy levels of TiO_2 conduction band, dyes, and I^-/I_3^- redox couple.

Generally, the photocurrent J_{SC} can be estimated from the incident photon-to-electron conversion efficiency (IPCE). Fig. 3a shows the IPCE curves as a function of the excitation wavelengths for these four dyes, which is critically dependent upon the inserted auxiliary group. To a great surprise, although the inserted EDOT unit can distinctly shift absorption to long wavelength, **WS-53** exhibited a very disappointed IPCE values (as low as 5%) across the whole visible range from 300-800 nm. In contrast, it is impressive that **WS-54** and **WS-55** bestows very broad and relatively high IPCE values. Upon increasing the electron-withdrawing capability of auxiliary

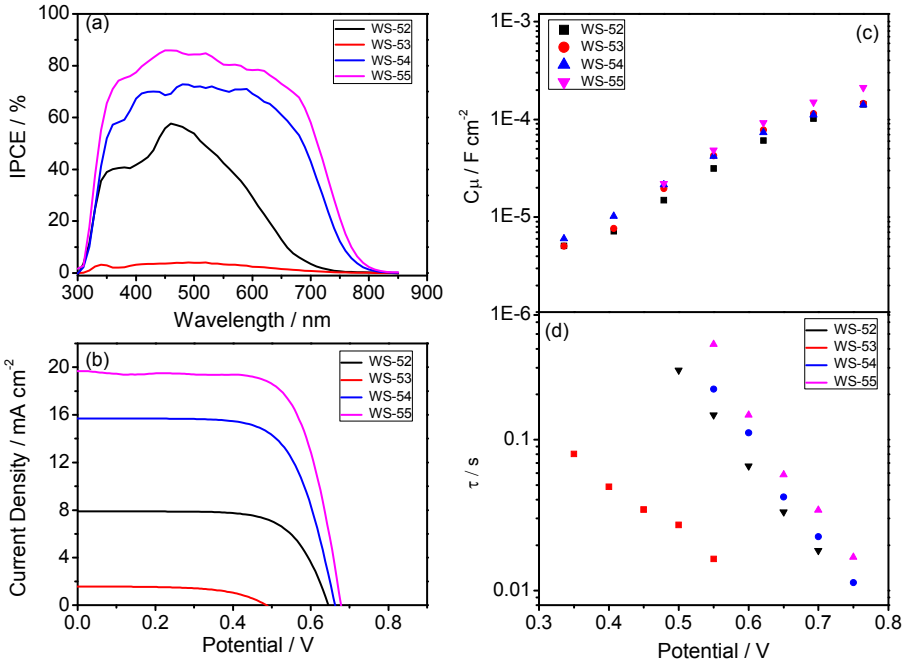

Fig. 3 IPCE (a), *J-V* curves (b), and bias potential against TiO_2 capacitance (c) and electron lifetime (d) in DSSCs sensitized by **WS-52**, **WS-53, WS-54** and **WS-55**.

group, the IPCE onset wavelength was extended step by step (Fig. 3a), from 730 nm for the reference dye **WS-52** and 800 nm for **WS-54** to 840 nm for **WS-55**, which is very uncommon for pure organic sensitizers. Among these four dyes, **WS-55** also showed the highest IPCE plateau with maximum value of 85.9%.

As known, the IPCE value is determined on the basis of four factors as follows: [5a]

$$\text{IPCE} = \text{LHE} \times \varphi_{inj} \times \varphi_{reg} \times \eta_{coll} \qquad \text{(Equation 1)}$$

Where LHE is the light-harvesting efficiency related to the incident light absorbed by dye molecules, φ_{inj} the electron injection efficiency from the excited dye molecules into TiO_2 conduction band, φ_{reg} the dye regeneration efficiency, and η_{coll} the collection efficiency of injected electrons to the FTO substrate. We took insight into these four factors to explore the different IPCE behaviors. Initially, the LHE spectra were calculated from the absorption spectra of the dye-loaded TiO_2 films (LHE = $1\text{-}10^{-\alpha}$, where α is the intensity of light absorption).[5a] As illustrated in Fig. 1c, the LHE curve for **WS-53** nearly reaches unity in the range of 400-600 nm, which is very similar to **WS-54** and **WS-55**. Obviously, the LHE effect on IPCE characteristics is almost same for **WS-53**, **WS-54** and **WS-55**. Based on the previously extensive studies through femtosecond transient absorption spectroscopy, when the driving force for electron injection from the excited dyes to nanoporous TiO_2 conduction band (-0.5 V vs. NHE, Fig. S1†) is greater than 0.2 V, the injection rate for many organic dyes is much faster than the rate of luminescence decay, and therefore the φ_{inj} is always considered to be almost unity, not the main handicap in the DSSC process.[9] Obviously, here the energy differences between LUMO and the TiO_2 conduction band for all these dyes are also sufficient (> 0.2 V), which can also guarantee the φ_{inj}. Also from EIS analysis, their electron collection efficiencies are found to be similar, around 90% at the bias potentials of 0.7 V (Fig. 1d).[10] Thus, the remaining effect is the dye regeneration efficiency (φ_{reg}). As shown in Fig. 2b, the HOMO energy levels for **WS-52**, **WS-54** and **WS-55** are 0.35, 0.41 and 0.50 V more positive than the Nernst potential of I^-/I_3^- electrolyte, respectively. All the driving forces are greater than 0.3 V, thus ensuring efficient dye regeneration. However, for **WS-53**, there existed only 0.17 V in the driving force to dye regeneration, which might heavily constrain the photocurrent as low as 1.22 mA cm^{-2}.

Moreover, based on the abovementioned Equation 1, once assuming that the φ_{inj} is unity one, the obtained φ_{reg} curves *vs.* wavelength were shown in Fig. S2†. In the 480-640 nm visible region, the electron-deficient auxiliary groups (BTD or BOD) have a powerful effect on the φ_{reg}, which almost reaches unity over 640 nm. With enhancement of the electron-withdrawing capability, it is very advantageous to the regeneration of the oxidation state dyes, which makes dye **WS-55** exhibit very good regeneration efficiency in this region within 0.9-1. However, the electron-rich group EDOT makes the φ_{reg} of **WS-53** sharply drop with the increase of wavelength. This result is extremely consistent with the low driving force to dye regeneration (0.17 V) for **WS-53**, along with a very poor photocurrent (1.22 mA cm^{-2}).

Apparently, among these four dyes, insertion of the electron-donating EDOT unit undesirably lifts up the HOMO energy level, resulting in a detrimentally insufficient driving force to dye regeneration. In contrast, the incorporation of electron-withdrawing BTD and BOD units can dramatically lower or deepen the LUMO orbital levels, resulting in narrow HOMO-LUMO gaps with preferable broad light response range. Given that BOD has stronger electron-withdrawing capability than BTD, we can step-by-step decrease the LUMO orbital level, and extend the light response range (Figs. 1b and 2a). In this way, upon the targeted modulation of LUMO levels, the photocurrent J_{SC} for **WS-53**, **WS-52**, **WS-54** and **WS-55** increased stepwise from 1.22, 7.88, 15.84 to 19.66 mA cm^{-2} (Table 1), respectively, which are well corresponding to the integrals of IPCE curves (1.17, 7.10, 14.43 and 19.56 mA cm^{-2}, Fig. S3†). In addition to the efficient level regulation action and high efficiency, the DSSCs based on **WS-55** also presented satisfactory photostability, remaining at 92% of the initial conversion efficiency after 500 h under visible-light irradiation (Fig. S4†).

Besides J_{SC}, **WS-53** also exhibits a low photovoltage (V_{OC}) of 440 mV, which is almost 200 mV lower than **WS-52**, **WS-54** and **WS-55**. As known, the alternation of photovoltage V_{OC} originates from a displacement of the electron quasi-Fermi-level (E_f) in TiO_2, which intrinsically stems from a change of TiO_2 conduction band edge (E_{CB}) and/or a fluctuation of electron density (charge recombination rate in DSSCs).[11] Considering that the chemical capacitance (C_μ) stands for the density of states in the bandgap of TiO_2, we plots the variation of capacitance at different bias potentials with the fitting of electrochemical impedance spectra (EIS, Fig. S5†) for illustrating the shift in the E_{CB} of TiO_2. Since these four dyes exhibited almost identical C_μ values (Fig. 3c), we can rule out the shift in TiO_2 conduction band as the main reason for the rather low photovoltage of **WS-53**. On the other hand, the fluctuation in TiO_2 electron density can also induce the difference in V_{OC}, which is closely related to the recombination resistance.[12] Fig. 3d illustrates the plots of electron lifetime under a series of potential bias, and the calculated electron lifetimes lie in the order as **WS-55** > **WS-54** > **WS-52** > **WS-53**, which is exactly consistent with the sequence of V_{OC}. Among these four dyes, the targeted LUMO and HOMO energy levels of **WS-55** is the most desirable. As a matter of fact, the auxiliary group change can distinctly increase the photovoltaic efficiency from EDOT (Dye **WS-53**, 0.24±0.06%), BDT (Dye **WS-54**, 7.14±0.09%) to BOD (Dye **WS-55**, 9.46±0.19%, obtained with the average of five cells listed in Fig. S6†). Under 0.3 sunlight irradiation, **WS-55** can even achieve a high PCE of 10.14% (Table 1 and Fig. S7†).

Conclusions

In summary, we have unprecedentedly targeted the customization of molecular energy levels with introducing auxiliary groups from electron donor to acceptor in D-π-A featured organic sensitizers. Dyes **WS-52**, **WS-53**, **WS-54** and **WS-55** exhibit well-modulated molecular energy levels in a stepwise manner, thus distinctly casting down the LUMOs, which are always too high in making energy "waste" for most practical organic dyes. As demonstrated, the photovoltaic efficiency is greatly improved when changing auxiliary group from EDOT (Dye **WS-53**, 0.24%), BDT (Dye **WS-54**, 7.14%) to BOD (Dye **WS-55**, 9.46%). Moreover, **WS-55** can even achieve a high PCE of 10.14% under 0.3 sunlight irradiation. It provides how the delicate balance in LUMO energy levels and HOMO-LUMO energy gaps guarantee the optimizing of photovoltaic properties.

Acknowledgements

This work was supported by NSFC for Creative Research Groups (21421004) and Distinguished Young Scholars (21325625), NSFC/China, Oriental Scholarship, Fundamental Research Funds for the Central Universities (WJ1416005 and WJ1315025), and Scientific Committee of Shanghai (14ZR1409700 and 15XD1501400) for financial support.

Notes and references

1 (*a*) B. O'Regan and M. Grätzel, *Nature*, 1991, **353**, 737–740; (*b*) D. J. Lipomi and Z. N. Bao, *Energy Environ. Sci.*, 2011, **4**, 3314–3328; (*c*) J. W. Shiu, Y. C. Chang, C. Y. Chan, H. P. Wu, H. Y. Hsu, C. L. Wang, C. Y. Lin and E. W. G. Diau, *J. Mater. Chem. A*, 2015, **3**, 1417–1420; (*d*) C. C. Chou, K. L. Wu, Y. Chi, W. P. Hu, S. J. Yu, G. H. Lee, C. L. Lin and P. T. Chou, *Angew. Chem. Int. Ed.*, 2011, **50**, 2054–2058; (*e*) L. Gao, J. Zhang, C. He, Y. Zhang, Q. J. Sun and Y. F. Li, *Sci. China Chem.*, 2014, **57**, 966–972; (*f*) M. Hoesel, H. F. Dam and F. C. Krebs, *Energy Tech.*, 2015, **3**, 293–304; (*g*) S. Ahmad, M. K. Nazeeruddin and J. Bisquert, *ChemPhysChem*, 2014, **15**, 987–989; (*h*) Y. Q. Wang, B. Chen, W. J. Wu, X. Li, W. H. Zhu, H. Tian and Y. S. Xie, *Angew. Chem. Int. Ed.*, 2014, **53**, 10779–10783; (*i*) S. W. Wang, K. L. Wu, E. Ghadiri, M. G. Lobello, S. T. Ho, Y. Chi, J. E. Moser, F. D. Angelis, M. Grätzel and M. K. Nazeeruddin, *Chem. Sci.*, 2013, **4**, 2423–2433; (j) Z. Sun, M. Liang and J. Chen, *Acc. Chem. Res.*, 2015, **48**, 1541–1550.

2 (*a*) L. Y. Han, A. Islam, H. Chen, C. Malapaka, B. Chiranjeevi, S. F. Zhang, X. D. Yang and M. Yanagida, *Energy Environ. Sci.*, 2012, **5**, 6057–6060; (*b*) A. Agrestia, S. Pescetellia, E. Gattob, M. Venanzib and A. D. Carloa, *J. Power Sources*, 2015, **287**, 87–95; (*c*) J. Zeng, T. L. Zhang, X. F. Zang, D. B. Kuang, H. Meier and D. R. Cao, *Sci. China Chem.*, 2013, **56**, 505–513; (*d*) Z. Y. Yao, M. Zhang, R. Z. Li, L. Yang, Y. N. Qiao and P. Wang, *Angew. Chem. Int. Ed.*, 2015, **54**, 5994–5998; (*e*) T. Higashino, Y. Fujimori, K. Sugiura, Y. Tsuji, S. Ito and H. Imahori, *Angew. Chem. Int. Ed.*, 2015, **54**, 9052–9056; (*f*) S. Mathew, A. Yella, P. Gao, R. Humphry-Baker, B. Curchod, N. Ashari-Astani, I. Tavernelli, U. Rothlisberger, M. K. Nazeeruddin and M. Grätzel, *Nat. Chem.*, 2014, **6**, 242–247.

3 (*a*) S. Ito, H. Miura, S. Uchida, M. Takata, K. Sumioka, P. Liska, P. Comte, P. Pechy and M. Grätzel, *Chem. Commun.*, 2008, 5194–5196; (*b*) B. Xu, H. Tian, L. Lin, D. Qian, H. Chen, J. Zhang, N. Vlachopoulos, G. Boschloo, Y. Luo, F. Zhang, A. Hagfeldt and L. Sun, *Adv. Energy Mater.*, 2015, **5**, 1401185; (*c*) R. Lin, H. Lin, Y. Yen, C. Chang, H. Chou, P. Chen, C. Hsu, Y. Chen, J. T. Lin and K. Ho, *Energy Environ. Sci.*, 2013, **6**, 2477–2486; (*d*) J. Liu, Y. Numata, C. J. Qin, A. Islam, X. D. Yang and L. Y. Han, *Chem. Commun.*, 2013, **49**, 7587–7589; (*e*) S. H. Kim, H. W. Kim, C. Sakong, J. Namgoong, S. W. Park, M. J. Ko, C. H. Lee, W. I. Lee and J. P. Kim, *Org. Lett.*, 2011, **13**, 5784–5787.

4 (*a*) Z. J. Ning, Q. Zhang, W. J. Wu, H. C. Pei, B. Liu and H. Tian, *J. Org. Chem.* 2008, **73**, 3791–3797; (*b*) M. D. Zhang, H. Xie, X. H. Ju, L. Qin, Q. Yang, H. G. Zheng and X. F. Zhou, *Phys.*, *Chem. Chem. Phys.* 2013, **15**, 634–641; (*c*) S. Namuangruk, R. Fukuda, M. Ehara, J. Meeprasert, T. Khanasa, S. Morada, T. Kaewin, S. Jungsuttiwong, T. Sudyoadsuk and V. Promarak, *J. Phys. Chem. C*, 2012, **116**, 25653–25663; (*d*) L. L. Tan, J. F. Huang, Y. Shen, L. M. Xiao, J. M. Liu, D. B. Kuang, C. Y. Su, *J. Mater. Chem. A*, 2014, **2**, 8988–8994; (*e*) B. Liu, B. Wang, R. Wang, L. Gao, S. H. Huo, Q. B. Liu, X. Y. Li, W. H. Zhu, *J. Mater. Chem. A*, 2014, **2**, 804–812.

5 (*a*) A. Hagfeldt, G. Boschloo, L. Sun, L. Kloo and H. Pettersson, *Chem. Rev.*, 2010, **110**, 6595–6663; (*b*) A. Mishra, M. K. R. Fischer, P. Bäuerle, *Angew. Chem. Int. Ed.*, 2009, **48**, 2474–2499; (*c*) M. Liang and J. Chen, *Chem. Soc. Rev.*, 2013, **42**, 3453–3488; (*d*) Y. Ooyama and Y. Harima, *Eur. J. Org. Chem.*, 2009, 2903–2934; (*e*) L. L. Li and E. W. G. Diau, *Chem. Soc. Rev.*, 2013, **42**, 291–304; (*f*) W. J. Ying, J. B. Yang, M. Wielopolski, T. Moehl, J. E. Moser, P. Comte, J. L. Hua, S. M. Zakeeruddin, H. Tian and M. Grätzel, *Chem. Sci.*, 2014, **5**, 206–214.

6 (*a*) Y. Z. Wu and W. H. Zhu, *Chem. Soc. Rev.* 2013, **42**, 2039–2058; (*b*) W. H. Zhu, Y. Z. Wu, S. T. Wang, W. Q. Li, X. Li, J. Chen, Z. S. Wang and H. Tian, *Adv. Funct. Mater.*, 2011, **21**, 756–763; (*c*) Y. Z. Wu, X. Zhang, W. Q. Li, Z. S. Wang, H. Tian and W. H. Zhu, *Adv. Energy Mater.*, 2012, **2**, 149–156; (*d*) Q. P. Chai, W. Q. Li, J. C. Liu, Z. Y. Geng, H. Tian and W. H. Zhu, *Sci. Rep.*, 2015, **5**, 11330; (*e*) W. Q. Li, B. Liu, Y. Z. Wu, S. Q. Zhu, Q. Zhang and W. H. Zhu, *Dyes Pigm.*, 2013, **99**, 176–184.

7 (*a*) X. F. Lu, Q. Y. Feng, T. Lan, G. Zhou and Z. S. Wang, *Chem. Mater.*, 2012, **24**, 3179–3187; (*b*) X. W. Kang, J. X. Zhang, D. O Neil, A. J. Rojas, W. Chen, P. Szymanski, S. R. Marder and M. A. El-Sayed, *Chem. Mater.*, 2014, **26**, 4486–4493; (*c*) J. Shi, J. N. Chen, Z. F. Chai, H. Wang, R. L. Tang, K. Fan, M. Wu, H. W. Han, J. G. Qin, T. Y. Peng, Q. Q. Li and Z. Li, *J. Mater. Chem.*, 2012, **22**, 18830–18838; (*d*) J. B. Yang, P. Ganesan, J. Teuscher, T. Moehl, Y. J. Kim, C. Yi, P. Comte, K. Pei, T. W. Holcombe, M. K. Nazeeruddin, J. L. Hua, S. M. Zakeeruddin, H. Tian and M. Grätzel, *J. Am. Chem. Soc.*, 2014, **136**, 5722–5730; (*e*) K. D. Seo, I. T. Choi, Y. G. Park, S. Kang, J. Y. Lee and H. K. Kim, *Dyes Pigm.*, 2012, **94**, 469–474.

8 (*a*) K. Hara, T. Sato, R. Katoh, A. Furube, Y. Ohga, A. Shinpo, S Suga, K. Sayama, H. Sugihara and H. Arakawa, *J. Phys. Chem. B*, 2003, **107**, 597–606; (*b*) T. Daeneke, A. J. Mozer, Y Uemura, S. Makuta, M. Fekete, Y. Tachibana, N. Koumura, U. Bach and L. Spiccia, *J. Am. Chem. Soc.*, 2012, **134**, 16925–16928.

9 (*a*) X. Xu, H. Wang, F. Gong, G. Zhou and Z. S. Wang, *ACS Appl. Mater. Interfaces*, 2013, **5**, 3219–3223; (*b*) Y. Tachibana, J. E. Moser, M. Grätzel, D. R. Klug and J. R. Durrant, *J. Phys. Chem.*, 1996, **100**, 20056–20062; (*c*) Y. Tachibana, S. A. Haque, I. P. Mercer, J. R. Durrant and D. R. Klug, *J. Phys. Chem. B*, 2000, **104**, 1198–1205; (*d*) J. B. Asbury, E. Hao, Y. Wang and T. Lian, *J. Phys. Chem. B*, 2000, **104**, 11957–11957; (*e*) B. O'Regan, J. Moser, M. Anderson and M. Grätzel, *J. Phys. Chem.*, 1990, **94**, 8720–8726.

10 S. Haid, M. Marszalek, A. Mishra, M. Wielopolski, J. Teuscher, J. Moser, R. Humphry-Baker, S. M. Zakeeruddin, M. Grätzel and P. Bäuerle, *Adv. Funct. Mater.*, 2012, **22**, 1291–1302.

11 (*a*) K. Pei, Y. Z. Wu, A. Islam, S. Q. Zhu, L. Y. Han, Z. Y. Geng and W. H. Zhu, *J. Phys. Chem. C*, 2014, **118**, 16552–16561; (*b*) W. Q. Li, Y. Z. Wu, Q. Zhang, H. Tian and W. H. Zhu, *ACS Appl. Mater. Interfaces*, 2012, **4**, 1822–1830.

12 F. Fabregat-Santiago, G. Garcia-Belmonte, I. Mora-Sero and J. Bisquert, *Phys. Chem. Chem. Phys.*, 2011, **13**, 9083–9118.

Unprecedentedly targeted customization of molecular energy levels with auxiliary-group in organic solar cell sensitizers

Yongshu Xie,‡ Wenjun Wu,‡ Haibo Zhu, Jingchuan Liu, Weiwei Zhang, He Tian and Wei-Hong Zhu*

Totally different: Casting down the LUMOs in decreasing energy "waste" is targeted through inserting an auxiliary group from electron donor to acceptor in D-π-A organic sensitizers. The variation of auxiliary group from 3,4-ethylenedioxythiophene to benzooxadiazole brings forth a distinct photovoltaic efficiency increase by 38 folds from 0.24 to 9.46%.